

# Design of weld fillers for mitigation of residual stresses in ferritic and austenitic steel welds

R. J. Moat<sup>1</sup>, H. J. Stone<sup>2</sup>, A. A. Shirzadi<sup>3</sup>, J. A. Francis<sup>4</sup>, S. Kundu<sup>2</sup>, A. F. Mark<sup>1</sup>, H. K. D. H. Bhadeshia<sup>2</sup>, L. Karlsson<sup>5</sup> and P. J. Withers<sup>\*1</sup>

Residual stresses that arise as a result of welding can cause distortion, and also have significant implications for structural integrity. Martensitic filler metals with low transformation temperatures can efficiently reduce the residual stresses generated during welding, because the strains associated with the transformation compensate for thermal contraction strains during cooling. However, it is vital that a low weld transformation temperature is not obtained at the expense of other important material properties. This article outlines the alloy design process used to develop appropriate low transformation temperature filler materials for the mitigation of residual stresses in both low alloy ferritic and austenitic stainless steel welds. Residual stresses in single pass, 6 mm bead in groove welds, on 12 mm thick plates, have been measured and compared against those obtained with commercially available conventional austenitic and ferritic filler materials. The filler metals developed here exceeded requirements in terms of weld mechanical properties, while significantly reducing the maximum residual stress in the weld and heat affected zone.

**Keywords:** Residual stress, Transformation plasticity, Low transformation temperature, Martensite

## Introduction

Residual stresses that arise as a consequence of welding can cause component distortion, and can have significant implications for structural integrity.<sup>1</sup> This paper explores the issues relating to the design of weld fillers that exploit martensitic transformations in order to mitigate the tensile residual stresses that are normally generated during the welding of ferritic and austenitic steels. This approach holds promise in engineering applications, such as for thick section power plant components, for which as-welded residual stresses are substantial and where post-weld on-site heat treatments may not be practical.

The efficacy of weld transformations for stress mitigation is strongly dependent on the martensite start temperature. If this is too high, the transformation will finish long before the weld has reached ambient temperature, and further tensile stress will accumulate due to thermal contraction of the martensite phase. Conversely, if the transformation temperature is too low, the transformation will be incomplete once the welded component reaches the room temperature, lessening the strain compensation effect. Wang *et al.*<sup>2</sup>

and Ohta *et al.*<sup>3,4</sup> successfully demonstrated the stress mitigating properties of low  $M_s$  martensitic filler materials by means of increased fatigue crack propagation resistance. However, this was achieved using alloys designed to have a low  $M_s$ , but to the detriment of fracture toughness (Charpy impact energy of just 20 J at 20°C), which limited the scope for the industrial application of their alloys. Murakawa *et al.*<sup>5</sup> made predictions for the optimal transformation temperature using finite element models which were supported by neutron diffraction measurements. It would appear from these studies that for single pass welds an  $M_s$  temperature that is approximately 200–250°C above the required preheat/interpass temperature can be extremely effective for the mitigation of tensile residual stresses.

The mitigation of weld residual stresses using transformation strains therefore poses an alloy design challenge.<sup>6</sup> On the one hand, the filler alloy must exhibit a low  $M_s$  temperature, which is fully exhausted on cooling to ambient temperatures. On the other hand, this must be achieved without sacrificing mechanical properties, such as toughness and resistance to the intended service environments. This has fuelled efforts to develop fillers for ferritic<sup>7</sup> and austenitic<sup>6</sup> welding applications with a good suite of properties.

In the present study, we discuss the design of filler alloys that exploit transformation-assisted stress mitigation using thermodynamic modelling to achieve the desired stress relief, but with weld microstructures that do not sacrifice mechanical properties (particularly toughness). The design process for two novel alloys is presented, one for a ferritic steel weld (to be referred to as the 'ferritic case') and one for a stainless steel weld

<sup>1</sup>School of Materials, Grosvenor St., Manchester, M1 7HS, UK

<sup>2</sup>Dept. of Materials Science & Metallurgy, Pembroke St, Cambridge, CB2 3QZ, UK

<sup>3</sup>Materials Engineering, The Open University, Walton Hall, Milton Keynes MK7 6AA, UK

<sup>4</sup>School of Mechanical, Aerospace and Civil Engineering, The University of Manchester, Manchester, M13 9PL, UK

<sup>5</sup>ESAB AB, Cent Res Labs, SE-40277 Gothenburg, Sweden

\*Corresponding author, email philip.withers@manchester.ac.uk

(to be referred to as the 'stainless case'). The performance of these fillers is examined for 12 mm thick, single pass groove welded plates, which are compared with welds made using conventional, commercially available filler materials.

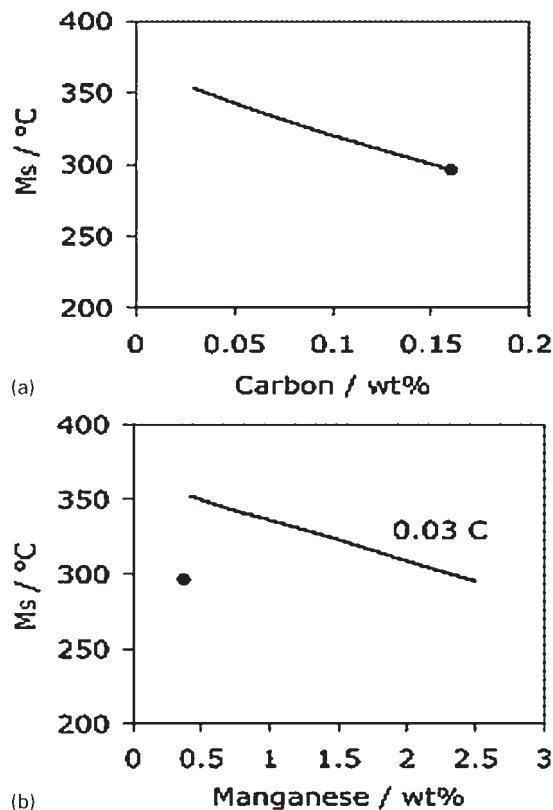
## Alloy design

For both the ferritic and stainless cases we identified existing alloys with some of the desired properties as starting points for the design process. For the ferritic case, the alloy proposed by Wang *et al.*<sup>2</sup> was identified, as it had a sufficiently low  $M_s$  (230 °C) however it exhibits poor fracture toughness (Charpy impact energy of 20 J at 20°C) which does not meet the recommended level for marine structures (27 J at -20°C).<sup>8</sup> For the austenitic case, a commercially available martensitic stainless weld filler alloy, OK84-52, was selected as it had suitable corrosion resistance and an  $M_s$  of ~250°C. The target properties of the new weld fillers are summarised in Table 1.

Many low  $M_s$  alloys devised to minimise residual stress suffer from low fracture toughness.<sup>2-4,6</sup> This is because the  $M_s$  may be lowered by increasing the carbon content (*see* Fig. 1a) and consequently a hard, brittle martensite is formed upon cooling. For a stainless steel, this also has the disadvantage of increasing chromium carbide formation, thereby increasing the susceptibility to corrosion.<sup>9,10</sup>

Other less detrimental strategies must be employed for lowering  $M_s$ . This means reducing the fraction of ferrite stabilisers or increasing the content of austenite stabilisers. Austenite stabilisers such as nickel and manganese can feasibly be increased in concentration. Chromium, although a ferrite stabiliser also reduces the  $M_s$ ,<sup>11</sup> however, modelling has shown that a high chromium content prevents full austenisation at high temperature,<sup>6</sup> counter to requirement (ii) (Table 1). For this reason the chromium content has been kept low in the ferritic case and at the minimum required content of 12.9 wt-% in the stainless case.

As part of the alloy development, a wide range of alloy compositions were modelled using thermodynamic and neural network predictions. The martensite start temperatures ( $M_s$ ) of some alloys with various concentrations of C, Ni, Cr and Mn were estimated using phase stability calculations and the thermodynamic databases of *plus* and *sub sgte*, which are linked to the MTDATA software package.<sup>6</sup> Example data sets calculated using MTDATA are shown in Fig. 1. Here it is clear how a reduction in carbon increases the  $M_s$  by ~50°C and how this can be counteracted by an increase of 2.5 wt-%Mn (Table 2).



1 Example results of thermodynamic (MTDATA) calculations of  $M_s$  with varying *a* carbon and *b* manganese content for stainless case (filled circle marker denotes composition of commercially available weld alloy OK84-52)<sup>6</sup>

In order to achieve an  $M_s$  in the desired range for the ferritic steel, the reduction in C content relative to the filler designed by Wang<sup>2</sup> is accompanied by an increase in nickel and a reduction in chromium concentration (Table 2). This was also determined by thermodynamic modelling in a similar fashion to that used for the stainless case. The new alloy (Series b) is predicted to have a  $M_s$  of 238°C as compared to 230°C for the Wang alloy, while neural network modelling also predicted that an increased Charpy impact energy should be achieved.

Thermodynamic modelling was also used to construct phase diagrams for the candidate alloys; this determined that the alloy solidifies as delta-ferrite, fully transforms to austenite and then transforms fully to martensite therefore confirming that the requirements (ii) and (iii) are fulfilled, as well as the requirement (iv) for the stainless case.

Table 1 Target weld alloy design criteria

Ferritic filler	Stainless filler
(i) $M_s \approx 200 \pm 50^\circ\text{C}$	(i) $M_s \approx 200 \pm 50^\circ\text{C}$
(ii) Fully austenitic at high temperatures	(ii) Fully austenitic at high temperatures
(iii) Transformation fully exhausted at ambient temperature	(iii) Solidify as delta-ferrite to prevent formation of low $T_m$ eutectics and to limit susceptibility to hot cracking.
(iv) Charpy impact energy equal to or greater recommended in Ref. 8 (27 J at -20°C).	(iv) Transformation fully exhausted at ambient temperature
	(v) Charpy impact energy equal to or greater recommended in Ref. 8 (27 J at -20°C).
	(vi) Maintain stainless character (>12.9 wt-%Cr)

A more detailed explanation of the modelling methodology used to derive the compositions for both the ferritic (Series b) and stainless (Camalloy) cases can be found in the literature.<sup>6,12</sup>

## Experimental

### Weld filler and weld manufacture

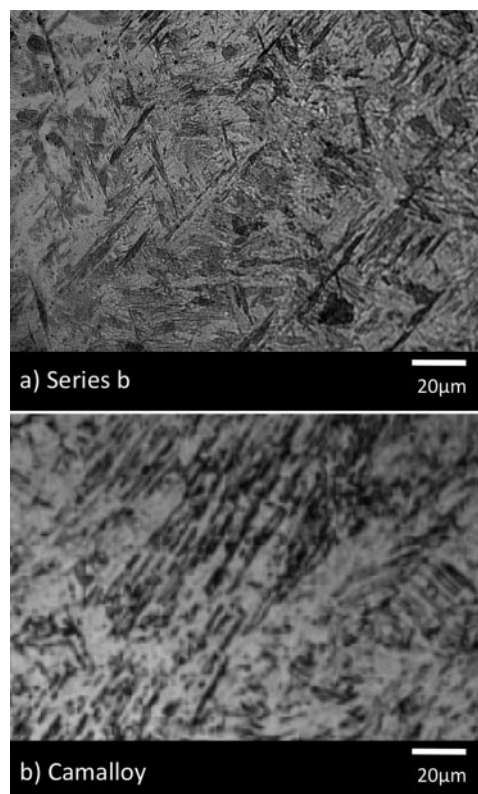
The new alloys were made in electrode form at ESAB<sup>13</sup> using the metal cored wire method. Nominally identical groove welds were produced using four different filler metals, comparing the performance of the two new filler materials directly alongside conventional filler metals. Two Weldox 90 plates 300 mm in length, 200 mm in width and 12 mm in thickness were welded using ferritic fillers (Series b and OK75-78) and two similar AISI grade 304L austenitic stainless steel plates were welded with stainless fillers (Camalloy and 308LSi). In each plate, a 6 mm deep 'V'-groove with an included angle of 60° was machined along the centre line of each 12 mm thick plate and a single weld bead was laid into each groove using the GMAW process. The plates were not fixed during this process.

### Satoh testing

Satoh tests<sup>14,15</sup> provide a straightforward means of characterising the capability for residual stress mitigation of the weld fillers during cooling. This was performed using 40 mm long matchstick samples with a cross-section of 1.5 × 1.5 mm in an Instron electrothermomechanical tester. Thermal cycles were applied using electrical resistance heating, monitored by an R-type thermocouple spot welded to the sample at the mid-length position. Cooling was achieved via water-cooled copper grips resulting in an approximately parabolic temperature distribution along the sample length, with the maximum temperature arising mid-length. Heating was carried out at 0 MPa, whereas during cooling the positions of the grips were constrained to allow the thermally induced stresses to accumulate. In each case the following thermal cycle was applied: heating to 850°C at 10°C s<sup>-1</sup>, holding for 60 s, cooling to room temperature at 10°C s<sup>-1</sup>.

### Residual stress measurement

Neutron diffraction is a well established means of measuring residual stress.<sup>16</sup> Precise details of the measurements are given elsewhere,<sup>7,17</sup> but in essence the transverse (T) and normal (N) measurements were made with 1 mm spatial resolution in the normal and transverse (N-T) directions while the longitudinal (L) strains (parallel to the welding direction) were measured with 2 mm spatial resolution. The stainless welds were studied on the SALS beam line, at the ILL<sup>18</sup> in Grenoble, France, using monochromatic, ~1.6 Å wavelength neutrons, analysing the {113} reflections



2 Micrographs of weld metal microstructure for a series b and b Camalloy revealed using Fry's reagent

from the austenite phase and the {112} ferritic/martensitic reflections. The ferritic welds were characterised on the L3 spectrometer, at the NRU reactor, Chalk River, Canada, using a monochromatic beam of 1.56 Å to record the {112} ferritic/martensitic reflections. Stress-free lattice parameters were determined from stress relieved 'comb' specimens extracted from the end of the welded plates using wire electrode discharge machining.<sup>19</sup> The lattice strains recorded in the three directions were used to calculate the corresponding residual stresses using well established formulae.<sup>16</sup> For the ferritic phase, the lattice specific elastic constants,  $E_{112}$  of 222 GPa and  $\nu_{112}$  of 0.277 were used, following Hauk,<sup>20</sup> and for the austenitic phase  $E_{113}$  of 184 GPa and  $\nu_{113}$  of 0.294 were used, following Webster *et al.*<sup>21</sup>

## Results and discussion

### Microstructures

The microstructures within the fusion zone were martensitic for both the Series b and Camalloy welds. The microstructures of these new weld alloys are shown in Fig. 2.

Table 2 Nominal composition of weld alloys (balance Fe), wt-%

	C	Si	Mn	Cr	Ni	Mo
OK84-52 (stainless filler starting point)	0.16	0.73	0.37	12.9	0.05	0.06
308LSi (non-transforming stainless filler)	<0.03	0.8	1.8	20.3	10.0	<0.3
Camalloy (new design stainless alloy)	0.01	0.73	1.5	13.0	6.0	0.06
Wang <i>et al.</i> (ferritic filler starting point)	0.07	0.20	1.3	9.1	8.5	...
OK75-78 (standard $M_s$ ferritic filler)	0.05	0.19	2.0	0.4	3.1	0.6
Series b (new design ferritic alloy)	0.03	0.65	0.5	1.0	12.0	0.5

## Mechanical performance

Charpy impact energies of 27 and 53 J (both at  $-20^{\circ}\text{C}$ ) were obtained for the ferritic and stainless cases respectively (see Table 3). While somewhat lower than the commercial fillers, the Charpy impact energy for Series b achieves and Camalloy exceeds the target values in Table 1. It is also clear that the yield stress of Camalloy is considerably higher than that for the benchmark non-transforming stainless filler due to the fine martensitic microstructure present in the Camalloy weld. The impact that mechanical property mismatches between filler and plates may have on the weld performance have not been characterised in this study but are of future interest.

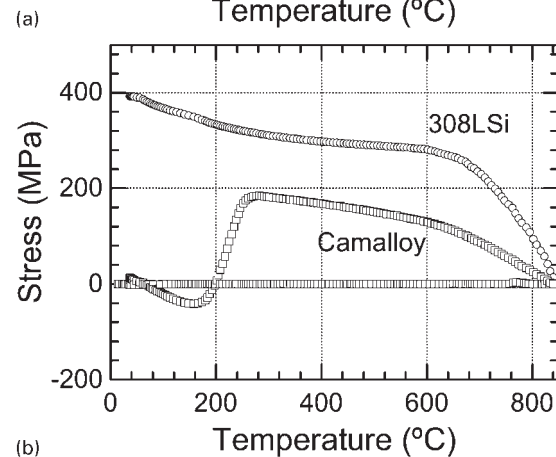
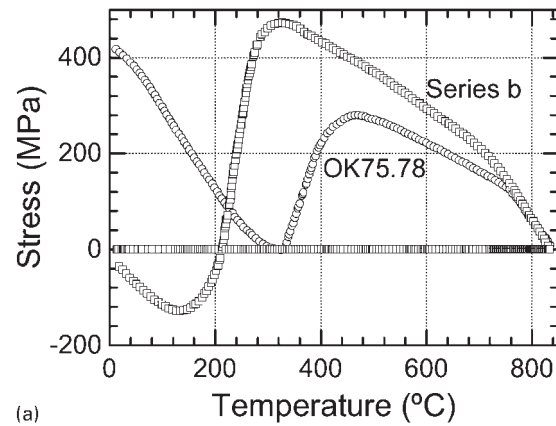
## Satoh tests

The Satoh responses for the ferritic and stainless case fillers are shown in Fig. 3, from which it is apparent that both new alloys significantly reduce the residual stresses relative to the benchmark weld metals. Since the 308LSi alloy does not transform during cooling, the continuous contraction of weld metal causes the stress to rise rapidly to the yield locus, which is then followed until room temperature is reached. By contrast, the new low  $M_s$  Camalloy shows a sudden drop in stress at  $\sim 280^{\circ}\text{C}$  due to the start of the martensitic transformation somewhere between the centre of the Satoh sample (i.e. the hottest point where the temperature was recorded) and the clamped ends. It must be noted that generally the temperature at which the sudden drop in stress is recorded does not represent the martensite start temperature of the alloy due to the presence of large temperature gradient along the Satoh samples.<sup>22</sup> As a consequence of the large transformation strain associated with the formation of martensite, the final stress at ambient temperature for Camalloy is  $\sim 20$  MPa, compared with  $\sim 390$  MPa for the non-transforming AISI grade 308LSi alloy.

Unsurprisingly, both ferritic fillers transform during cooling (Fig. 2a) starting at approximately  $440^{\circ}\text{C}$  for OK75-78 and  $320^{\circ}\text{C}$  for the Series b alloy. The transformations appear to exhaust around 320 and  $150^{\circ}\text{C}$  respectively for the two alloys, beyond which the tensile thermal contraction stresses begin to recover leading to room temperature residual stresses in the vicinity of  $\sim 430$  MPa and about  $-30$  MPa.

## Residual stresses in welded plates

The residual stresses in the welded plates are shown in Fig. 4. For the conventional stainless filler (Fig. 4a), the weld filler fusion zone is characteristically in longitudinal tension ( $\sim 600$  MPa). Indeed, as one would expect, the localised heating of the parent below the groove has also introduced tensile stresses there. In the transverse direction, the residual stresses are low

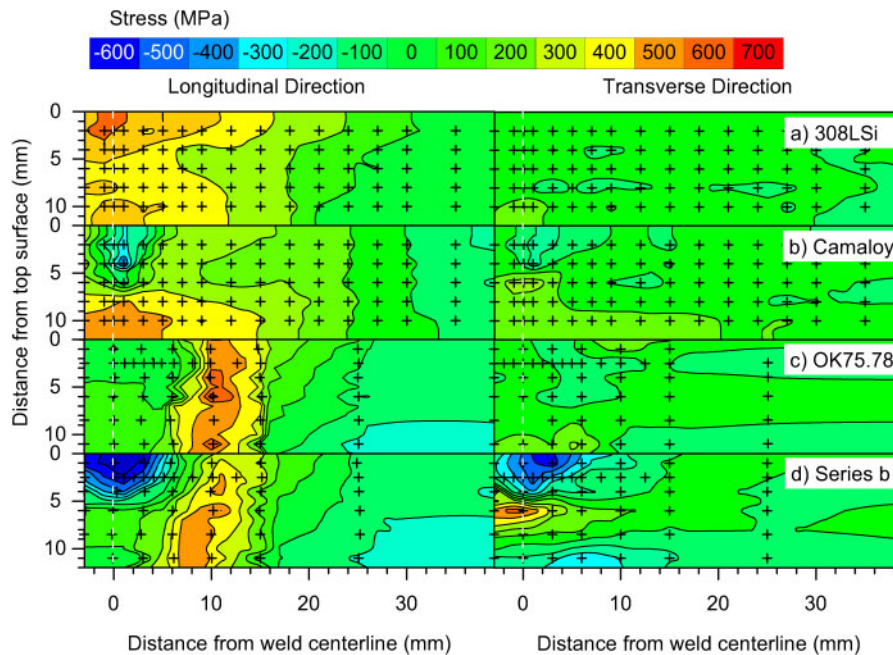


3 Satoh test samples cooled (at  $10^{\circ}\text{C s}^{-1}$ ) from  $850^{\circ}\text{C}$  to room temperature for a OK75-78 and Series b (ferritic case) and b 308LSi and Camalloy (stainless case)

compared to the longitudinal direction with stresses not exceeding 200 MPa. In contrast, the fusion zone for the plate welded with the Camalloy low transformation temperature stainless filler (Fig. 4b) is compressively stressed, reaching  $-420$  MPa. The longitudinal stresses become approximately zero at the fusion boundary and reach a maximum of  $\sim 460$  MPa in the non-transforming plate beneath the groove. Laterally the maximum stress near the top surface is around 8 mm from the weld centreline ( $\sim 350$  MPa). In this case, because the parent plate cannot transform, the compressive longitudinal stresses are confined to the fusion zone. In the transverse direction, the fusion zone is somewhat less compressively stressed reaching  $-320$  MPa. Just below the fusion zone there is a small lobe of tensile stress reaching 280 MPa, which is in reaction to the slight bending moment setup by the transforming weld metal. This differs from the AISI grade 308LSi weld because no local bending is experienced in the absence of a transformation.

Table 3 Mechanical properties and transformation temperatures<sup>6,12</sup>

	Yield stress/MPa	Charpy energy <sup>23</sup> /J		$M_s/^{\circ}\text{C}$	
		$-20^{\circ}\text{C}$	$20^{\circ}\text{C}$	Expt/(modelled)	$B_s/^{\circ}\text{C}$
308LSi	370	95	110	...	...
Camalloy	838	53	72	216/(232)	...
304Li (baseplate)	310	175	...	...	...
OK75-78	$\sim 1000$	90	96	400	410
Series b	$\sim 1100$	27	28	250/(238)	...
Weldox 960 (baseplate)	$>960$	27-30	28-34	370	460



4 (LHS) Longitudinal and (RHS) transverse residual stress distributions for the T-N section at the weld mid length. Crosses denote measurement locations and white dashed line denotes weld centre line. Only the central region of interest is shown here; approximate - stress balance was observed over the whole weld section

In the plate welded with ferritic OK75.78 (Fig. 4c), the residual stress varies relatively little with depth within 15 mm of the centreline. This is because the parent and filler metals have similar transformation temperatures (Table 3) and the thermal profile varies little through-thickness. Just beyond the region heated above the  $A_{c3}$  temperature a steep increase in stress is observed reaching almost 800 MPa.

There are several key differences between the residual stresses for the plate with an OK75.78 weld metal and those made with the new alternative Series b filler metal (Fig. 4d). Most noticeably, in the fusion zone of the Series b weld the residual stresses are significantly more compressive throughout, reaching  $-570$  MPa. The stresses in the parent material immediately below the groove are similar in magnitude to those observed for the weld made with the OK75.78 filler metal. Meanwhile, the maximum tensile stresses, which are located  $\sim 10$  mm from the weld centre line, are significantly lower than those for the OK75.78 weld reaching just 580 MPa. Low transverse stresses were found for the weld made with the standard filler metal (OK75.78) because the start temperature is essentially the same for the fusion zone and the underlying base metal and therefore the transformations do not induce any local bending. The Series b weld has a region of compressive stress in the fusion zone with a lobe of tensile stress ( $\sim 570$  MPa) just below the weld zone. In this case the transformation in the HAZ will have exhausted by the time the fusion zone transforms and will therefore introduce a similar local bending stress to that which was observed in the Camalloy weld.

In both cases the use of a low temperature transformation filler metal has reduced the longitudinal and transverse stresses in the fusion zone as well as in the surrounding HAZ, at depths which correspond to the depth of the fusion zone. Maximum longitudinal tensile stresses of 410 and 260 MPa were measured in the top 3 mm of the welded plate for Series b and Camalloy

respectively. That is a reduction in stress compared to the standard commercial alloy of  $\sim 150$  MPa for both respective alloys. A reduction in surface stresses could be particularly advantageous for the stainless case, since the near-surface stresses will be particularly pertinent to the possibility of degradation through environmentally assisted cracking. The two low  $M_s$  fillers also introduce tensile transverse stresses just below the fusion zone that are not found for the conventional fillers. The magnitudes of these stresses were notably less than the maxima in stress in the longitudinal direction.

## Conclusions and future work

Using thermodynamical phase prediction software it has been possible to design low  $M_s$  temperature ferritic low alloy and stainless steel weld filler metals that have good toughness and in the latter case a chromium content sufficient to satisfy the corrosion resistance requirement. Furthermore, these low  $M_s$  weld fillers have been shown to introduce compressive longitudinal and transverse residual stresses into the fusion zone of welds. Depending on the requirements it would also be possible to design weld fillers that lead to little or no longitudinal residual stress in the weld bead using the same approach.

This study has examined the simple case of single bead welds; in many industrial applications multiple weld beads will be required. Further work is required to investigate the performance of such weld fillers in multipass weldments. This is pertinent because it is often the case that thick multipass welds are difficult to post-weld heat treat and, as such, these welds stand to benefit significantly from low  $M_s$  fillers. One course of investigation being followed at present is the use of a holding (or interpass) temperature during multipass welding. It is anticipated that weld preheat and interpass temperatures in excess of the  $M_s$  temperature could be used to advantage to control the onset of transformation.

## Acknowledgement

The authors are grateful for financial support from the UK Ministry of Defence and the provision of beam time at the ILL and NRU.

## References

1. P. J. Withers: 'Residual stress and its role in failure', *Rep. Prog. Phys.*, 2007, **70**, (12), 2211.
2. W. X. Wang, L. X. Huo, Y. F. Zhang, D. P. Wang and H. Y. Jing: 'New developed welding electrode for improving the fatigue strength of welded joints', *J. Mater. Sci. Technol.*, 2002, **18**, 527–531.
3. A. Ohta, N. Suzuki, Y. Maeda, K. Hiraoka and T. Nakamura: 'Superior fatigue crack growth properties in newly developed weld metal', *Int. J. Fatigue*, 1999, **21**, 113–119.
4. A. Ohta, K. Matsuoka, N. T. Nguyen, Y. Maeda and N. Suzuki: 'Fatigue strength improvement of lap joints of thin steel plate using Low-transformation-temperature welding wire', *Weld. J.*, 2003, **82**, 78–83.
5. H. Murakawa, M. Beres, C. M. Davies, S. Rashed, A. Vega, M. Tsunori, K. M. Nikbin and D. Dye: 'Effect of low transformation temperature weld filler metal on welding residual stress', *Sci. Technol. Weld. Join.*, 2010, **15**, (5), 393.
6. A. A. Shirzadi, H. K. D. H. Bhadeshia, L. Karlsson and P. J. Withers: 'Stainless steel weld metal designed to mitigate residual stresses', *Sci. Technol. Weld. Join.*, 2009, **14**, 559–565.
7. J. A. Francis, H. J. Stone, S. Kundu, R. B. Rogge, H. K. D. H. Bhadeshia, P. J. Withers and L. Karlsson: 'The effects of filler metal transformation temperature on residual stresses in a high strength steel weld', *J. Press. Vessel Technol.*, 2009, **131**, 041401.
8. J. D. G. Sumpter and A. J. Caudrey: 'Recommended fracture toughness for ship hull steel and weld', *Marine Struct.*, 1994, **8**, 345–357.
9. A. P. Bond: 'Mechanisms of intergranular corrosion in ferritic stainless steels', *Trans. Metall. Soc. AIME*, 1969, **245**, 2127–2134.
10. T. Sourmail, C. H. Too and H. K. D. H. Bhadeshia: 'Sensitisation and evolution of Cr-depleted zones in Fe-Cr-Ni-C systems', *ISIJ Int.*, 2003, **43**, 1814–1820.
11. C. Capdevila, F. G. Caballero and C. Garcia De Andres: 'Determination of  $M_s$  temperature in steels: a Bayesian neural network', *ISIJ Int.*, 2002, **42**, (8), 894–902.
12. S. Kundu: PhD thesis, 'Transformation Strain and Crystallographic Texture in Steels', University of Cambridge, Cambridge, UK, 2007.
13. ESAB: Personal communication.
14. K. Satoh: 'Transient stresses of weld heat-affected zone by both-ends-fixed bar analogy', *Trans. Jpn Weld. Soc.*, 1972, **3**, 125–134.
15. K. Satoh: 'Thermal stress developed in high strength steels subjected to thermal cycles simulating weld heat-affected-zone', *Trans. Jpn Weld. Soc.*, 1972, **3**, 135–142.
16. M. T. Hutchings, P. J. Withers, T. M. Holden and T. Lorentzen: 'Introduction to the characterization of residual stress by neutron diffraction', 2005, Boca Raton, FL, CRC Press.
17. H. Dai, A. F. Mark, R. Moat, A. A. Shirzadi, H. K. D. H. Bhadeshia, L. Karlsson and P. J. Withers: 'Modelling of Residual Stress Minimization through Martensitic Transformation in Stainless Steel Welds', In: *Mathematical Modelling of Weld Phenomena 9*. Cerjak H, Enzinger N, editors. Graz: Verlag der Technischen Universität Graz, 2010, p.239–252.
18. T. Pirling, G. Bruno and P. J. Withers: 'SALSA – a new instrument for strain imaging in engineering materials & components', *Mater. Sci. Eng. A*, 2006, **A437**, 139–144.
19. P. J. Withers, M. Preuss, A. Steuwer and J. W. L. Pang: 'Methods for obtaining a strain free lattice parameter when using diffraction to determine residual stress', *J. Appl. Crystallogr.*, 2007, **40**, 891–904.
20. V. Hauk: 'Structural and residual stress analysis by nondestructive methods', 1997, New York, Elsevier.
21. P. J. Webster, G. Mills, D. X. Wang, X. D. Kang and T. M. Holden: 'Neutron strain scanning of a small welded austenitic stainless steel plate', *J. Strain Anal.*, 1995, **30**, (1), 35–43.
22. A. A. Shirzadi and H. K. D. H. Bhadeshia: 'Accumulation of stress in constrained assemblies: novel Satoh test configuration', *Sci. Technol. Weld. Join.*, 2010, **15**, (6), 479–499.
23. 'Metallic materials – Charpy pendulum impact test – Part 1: test method ISO 148-1', Swedish Standards Institute, Sweden, 2009.